Segregated Phases in Pulmonary Surfactant Membranes Do Not Show Coexistence of Lipid Populations with Differentiated Dynamic Properties

Jorge Bernardino de la Serna,[†] Greger Orädd,[‡] Luis A. Bagatolli,[§¶] Adam C. Simonsen,[¶] Derek Marsh,[‖] Göran Lindblom,[‡] and Jesus Perez-Gil[†*]

[†]Universidad Complutense, Departmento de Bioquimica, Facultad de Biologia Biologia, 28040 Madrid, Spain; [‡]Umeå University, Umeå, Sweden; [§]Membrane Biophysics and Biophotonics Group, Department of Biochemistry and Molecular Biology, and [¶]MEMPHYS-Center for Biomembrane Physics, Department of Physics and Chemistry, University of Southern Denmark, Odense, Denmark; and [‖]Max-Planck-Institut für biophysikalische Chemie, Abteilung Spektroskopie, Göttingen, Germany

ABSTRACT The composition of pulmonary surfactant membranes and films has evolved to support a complex lateral structure, including segregation of ordered/disordered phases maintained up to physiological temperatures. In this study, we have analyzed the temperature-dependent dynamic properties of native surfactant membranes and membranes reconstituted from two surfactant hydrophobic fractions (i.e., all the lipids plus the hydrophobic proteins SP-B and SP-C, or only the total lipid fraction). These preparations show micrometer-sized fluid ordered/disordered phase coexistence, associated with a broad endothermic transition ending close to 37°C. However, both types of membrane exhibit uniform lipid mobility when analyzed by electron paramagnetic resonance with different spin-labeled phospholipids. A similar feature is observed with pulse-field gradient NMR experiments on oriented membranes reconstituted from the two types of surfactant hydrophobic extract. These latter results suggest that lipid dynamics are similar in the coexisting fluid phases observed by fluorescence microscopy. Additionally, it is found that surfactant proteins significantly reduce the average intramolecular lipid mobility and translational diffusion of phospholipids in the membranes, and that removal of cholesterol has a profound impact on both the lateral structure and dynamics of surfactant lipid membranes. We believe that the particular lipid composition of surfactant imposes a highly dynamic framework on the membrane structure, as well as maintains a lateral organization that is poised at the edge of critical transitions occurring under physiological conditions.

INTRODUCTION

The lungs of air-breathing vertebrates must cope with a delicate balance of physical forces derived both from the exposure of a large surface for gas exchange with the environment, and from the presence at such surfaces of a thin layer of aqueous fluid. Thus, the respiratory epithelium has evolved to produce and secrete a lipid-protein complex, pulmonary surfactant, the main function of which is to reduce the surface tension at the respiratory air-liquid interface, stabilizing the lungs against physical forces tending to collapse (1,2); ~80% by mass of surfactant is phospholipids, which are stored in pneumocytes in the form of tightly packed bilayers, whose unpacking on secretion and efficient adsorption at the alveolar interface requires the presence of a pair of specialized hydrophobic proteins, SP-B and SP-C (3). These proteins, each constituting <1% by mass of surfactant, facilitate rapid movement of surfactant phospholipids to spaces close to the air-liquid interface and their efficient transfer from bilayers to the interface. Lack of, or alteration in, surfactant is associated with severe respiratory pathologies (4). Pulmonary surfactant films are particularly enriched in phospholipid species bearing saturated acyl chains, such as dipalmitoylphosphatidylcholine (DPPC), which accounts for ~40% of surfactant by mass in most animal species (5). Another 25% of surfactant consists of unsaturated phosphatidylcholine species and 15% is composed of anionic phospholipids, which are involved in lipid-protein interactions with the cationic segments of surfactant proteins SP-B and SP-C (6). To complete pulmonary surfactant lipid composition, proportions of ~5–10% by weight are taken up by neutral lipids, mainly cholesterol.

Current models propose that saturated and unsaturated phospholipid species are integrated in surfactant membranes and films to form a complex heterogeneous structure. Some membrane and monolayer regions (domains) accumulate and segregate saturated phospholipid species, mainly DPPC (7), which are suited to support the highest pressures occurring at the end of expiration. On the other hand, regions in surfactant membranes enriched in unsaturated phospholipid species, where the hydrophobic surfactant proteins partition, could provide suitable environments for the structural transformations associated with reversible bilayer-monolayer transitions (reviewed in Perez-Gil (8)). Interestingly, a thermotropic transition occurs in surfactant membranes at around physiological temperatures, which disorders a substantial proportion of the ordered, presumably DPPC-enriched, regions in both membranes (9) and interfacial monolayers (10). It has been argued, therefore, that the lateral structure of surfactant membranes could be specially optimized to sustain dynamic performance under physiological conditions

Submitted February 10, 2009, and accepted for publication June 23, 2009.

This paper is dedicated to the memory of Maria Luisa de la Serna.

*Correspondence: jpg@bbm1.ucm.es

Jorge Bernardino de la Serna's present address is MEMPHYS-Center for Biomembrane Physics, Department of Physics and Chemistry, University of Southern Denmark, Odense, Denmark.

Editor: Paul H. Axelsen.

0006-3495/09/09/1381/9 $2.00

doi: 10.1016/j.bpj.2009.06.040

(11). So far, however, few studies have addressed the dynamic and thermotropic properties of phospholipids in surfactant membranes under physiologically relevant conditions.

The main goal of this study is to characterize the dynamic parameters of phospholipids and their temperature dependence in native surfactant membranes and in membranes reconstituted from various surfactant components.

MATERIALS AND METHODS

Materials

Fluorescent probes, 1,1-dioctadecyl-3,3,3,3-tetramethylindocarbocyanine perchlorate (DiIC18), 2-(4,4-difluoro-5,7-dimethyl-4-bora-3*a*, 4*a*-diaza-*s*indacene-3-pentanoyl)-1-hexadecanoyl-*sn*-glycero-3-phosphocholine (Bodipy-PC), and 6-lauroyl-2-(*N*,*N*-dimethylamino)naphthalene (LAURDAN) were from Molecular Probes (Invitrogen, Copenhagen, Denmark). Spin-labeled stearic acid and phosphatidylcholine with the nitroxide group at different positions in the *sn*-2 acyl chain were synthesized as described in Marsh and Watts (12).

Native pulmonary surfactant (NPS) was isolated from bronchoalveolar lavage fluid as described previously (13). Native pulmonary surfactant extract (NPSE) was obtained by chloroform/methanol extraction and contains all lipid species plus the hydrophobic proteins SP-B and SP-C. The whole lipid fraction (NPSL) was obtained by removing protein from phospholipid and neutral lipid components of NPSE with Sephadex LH-20 chromatography, as described and analyzed elsewhere (14). Fractionation of NPSE in LH-20 under the conditions proposed by Discher and co-workers (15) allowed obtention of the protein-free and cholesterol-free phospholipid fraction (NPSP) of surfactant. The lipid composition of the different fractions is described elsewhere. NPSL and NPSP fractions contained no detectable protein, as assessed by electrophoresis and amino acid analysis.

Differential scanning calorimetry

Differential scanning calorimetry (DSC) analysis of NPS or the multilamellar suspensions of NPSE, NPSL, or NPSP in 150 mM NaCl, 5 mM Tris buffer pH 7, was carried out in a MicroCal VP-DSC (Northampton, MA) microcalorimeter. Samples contained 15 mM total phospholipid concentration and the scan rate was 0.5 K/min, with buffer in the reference cell. Five temperature scans between 15°C and 60°C were collected from each sample. The calorimetric experiments were repeated at least three times with two different sets of samples, and the results were comparable, with enthalpy variations of $<10\%$ from sample to sample. Data presented correspond to illustrative experiments carried out with a coherent set of samples, originating from the same surfactant starting material.

Confocal and two-photon excitation fluorescence microscopy

Giant unilamellar vesicles (GUVs) were used for fluorescence microscopy experiments. A small trace (0.1 mol %) of lipophilic fluorescent probe ($DiIC_{18}$, Bodipy-PC, or LAURDAN) was incorporated into the giant vesicles. Conditions for observation were described previously (9). Changes in shape and size of microdomains produced on illumination were never observed in GUVs made of the natural samples studied here. A Zeiss LSM 510 META NLO microscope (Carl Zeiss, Jena, Germany) was used in one- or two-photon excitation modes. Excitation wavelengths used were 488 nm (Bodipy-PC), 543 nm (DiIC18), and 780 nm (LAURDAN under two-photon excitation mode).

LAURDAN GP images were obtained following the general procedure described previously (16), using fluorescence intensity images obtained simultaneously in the blue and red regions of the emission spectrum (band-pass filters 428 ± 37 nm and 515 ± 15 nm, respectively).

Electron paramagnetic resonance spectroscopy

The required spin-labeled lipid was incorporated into surfactant preparations at a level of 1 mol%. NPS was labeled from a trace volume of methanol, followed by washing to remove nonincorporated probe and residual solvent. Surfactant extracts, NPSE, NPSL, and NPSP, were doped with the spin-labeled lipid in $CHCl_3$/MeOH (2:1, v/v), before drying and suspending in 100 μL of 150 mM NaCl, 5 mM Tris buffer, pH 7. Samples were pelleted in the 100-μL capillary tubes used for electron paramagnetic resonance (EPR) spectroscopy by centrifugation at 3000 rpm in a bench centrifuge. EPR spectra were recorded with a Bruker 9-GHz EMX spectrometer equipped with a nitrogen gas-flow temperature regulation system. See Perez-Gil et al. (17) for details of spectral analysis. Figures represent illustrative data after repeating the experiments with independently purified batches of native pulmonary surfactant fractions, which showed similar qualitative behavior and comparable quantitative hyperfine splittings.

Pulsed field gradient NMR

Macroscopically oriented lipid or lipid-protein bilayers were prepared with excess water as reported previously (18). The ^{31}P-NMR lineshape gave a lower estimate for the degree of alignment, which varied from 65% to 85%. Measured lipid diffusion coefficients did not depend on the degree of alignment. Diffusion measurements were carried out on a Chemagnetics Infinity NMR spectrometer operating at a proton frequency of 400 MHz and equipped with a specially designed goniometer probe that enabled macroscopically aligned bilayers to be oriented with the bilayer normal at the magic angle (54.7°) with respect to the static magnetic field. This procedure eliminates dipolar interactions that would otherwise obscure the diffusion measurement. Temperature was controlled to within ±0.5°C by a heated air stream passing the sample. The stimulated spin-echo pulse sequence was used (19), in which the field gradient amplitude was varied while keeping all other parameters constant. Data were analyzed with the CORE method for global analysis of the entire data set (20). The analysis identified one fast component originating from water and one slow component assigned to the phospholipids. Because of spectral overlap of the resonances from different lipids, no assignment can be made to specific lipid components. Detailed discussion of the data analysis (e.g., the conditions for a lipid diffusion decay to consist of one or two components) can be found in Oradd and Lindblom (21). Measurements were carried out in the temperature range 20–60°C, starting from the highest temperature. At each temperature, two diffusion experiments were carried out, in which the diffusion time, Δ, was 15 and 100 ms, respectively. The diffusion coefficients obtained did not depend on the value of Δ.

RESULTS

It has been shown recently that membranes from native pulmonary surfactant exhibit coexistence of liquid-ordered and liquid-disordered regions, with a thermotropic transition close to physiological temperatures (9). Fig. 1 compares DSC thermograms of the four membrane preparations used in this study. All thermograms display a broad asymmetric endothermic peak, with a maximum at ~32°C and a relatively sharp completion at temperatures slightly above 37°C. Similar scans were obtained previously from animal surfactant preparations (22) and confirm that the lipid component of surfactant is mainly responsible for the transition associated with phase separation, because NPSL membranes behave similarly to NPS or NPSE membranes. NPSP membranes reconstituted from the phospholipid fraction depleted of cholesterol show a sharper thermotropic transition, which is completed by 37°C.

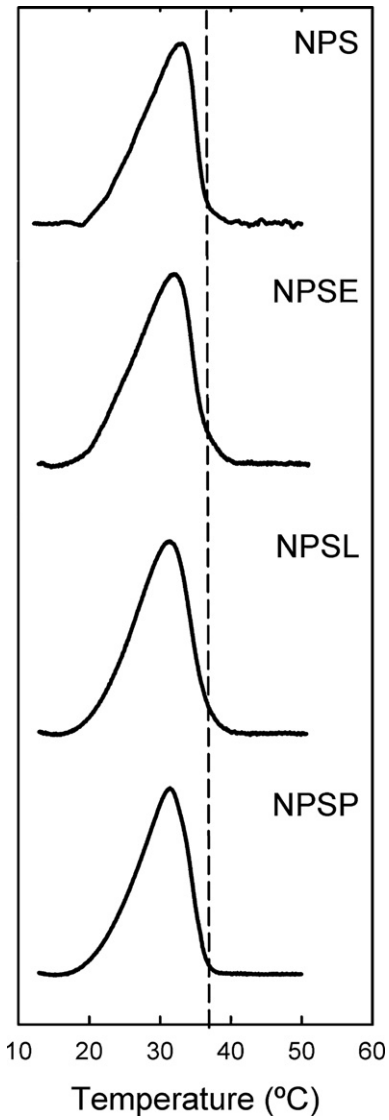

FIGURE 1 Thermotropic behavior of native pulmonary surfactant and membranes reconstituted from its fractions. DSC thermograms were obtained from suspensions of native pulmonary surfactant purified from porcine lungs (NPS), or reconstituted from surfactant organic extract containing all the lipids and the hydrophobic proteins (NPSE), the whole lipid fraction of surfactant depleted of proteins (NPSL), or the phospholipid fraction of surfactant (NPSP) resulting from removal of proteins and neutral lipids from the organic extract. Suspensions with 1 mg/mL phospholipid concentration were scanned at 0.5 K/min. The dashed line marks 37°C.

Table 1 gives the thermodynamic parameters of the thermotropic transitions in the different surfactant membranes studied. All the samples exhibit a relatively low enthalpy, on the order of 2–3 kcal/mol, associated with the transition from ordered to disordered phases. For comparison, the chain-melting enthalpy of pure DPPC membranes is ~7.5 kcal/mol. The lower enthalpy for surfactant membranes is therefore more characteristic of a fluid-fluid transition than a gel-fluid transition (e.g., Marsh (23)). Protein-containing membranes show transitions with somewhat lower enthalpies, ~2 kcal/mol, than those of protein-free membranes, which are

TABLE 1 Thermodynamic parameters of the calorimetric transition of native pulmonary surfactant and its reconstituted fractions

	ΔH (kcal/mol)	T_m (°C)	$\Delta T_{1/2}$ (°C)
NPS	2.1	33.2	8.7
NPSE	1.9	32.0	9.2
NPSL	3.3	31.4	9.0
NPSP	2.6	30.2	8.0

~3 kcal/mol. Lipid-protein interactions with surfactant proteins SP-A, SP-B, and SP-C therefore reduce the total enthalpy of transition per mol of lipids, presumably because of perturbation of the transition for lipids in contact with the proteins.

Confocal microscope images of GUVs composed of the different surfactant materials confirm that increasing temperature causes transition of a substantial proportion of microscopic-sized ordered-like domains (Fig. 2). Membranes of GUVs from NPS, NPSE, or NPSL show a coexistence of two liquid phases at temperatures below 37°C. These consist of disordered-like domains (*yellow-green*, labeled with Bodipy-PC), presumably enriched in unsaturated phospholipid species (~25% of total lipid), dispersed in a background of an ordered-like phase (*red*, labeled with DiIC18), presumably enriched in DPPC (~40% of total surfactant mass). Membranes of NPSP show a completely different morphology, which is consistent with a gel/fluid type of coexistence, although the total transition enthalpy is much too low for such a transition. Heating GUVs to temperatures above physiological (i.e., to 40°C) results in disappearance of most of the ordered phase, yielding a lateral structure dominated by a presumably liquid-disordered phase but containing a minor fraction of lipids in which the fluorescent probes have only limited solubility, and whose composition and order/packing are difficult to infer.

To obtain further insight into the properties of the phases segregated in surfactant membranes we have recorded confocal fluorescence images under two-photon excitation conditions of GUVs doped with traces of the probe LAURDAN (Fig. 3). LAURDAN partitions evenly in membranes displaying phase coexistence, and its emission is highly sensitive to the extent of water dipolar relaxation of the local probe environment, which in turn depends on lipid packing. Images in Fig. 3 show segregation of ordered and disordered phases observed at 20°C in NPS, NPSE, and NPSL membranes, revealed by differences in the LAURDAN generalized polarization (GP). Table 2 summarizes the values of LAURDAN GP determined from the two types of phases. In the three types of membranes, the more ordered phase shows LAURDAN fluorescence with similar GP values of ~0.34–0.36, coexisting with regions of a significantly lower GP, in the range 0.07–0.11 that is characteristic of a more disordered phase. These values of GP are typical for liquid-ordered/liquid-disordered phase coexistence, as determined in simple binary and ternary cholesterol-containing lipid mixtures (24).

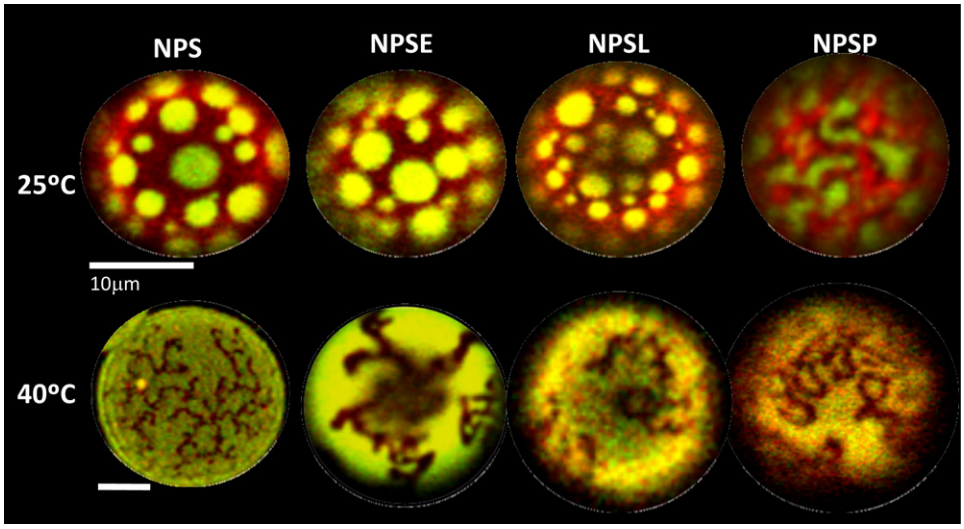

FIGURE 2 Effect of temperature on phase segregation in native pulmonary surfactant and membranes reconstituted from its fractions Segregation of phases at temperatures below (25°C) and above (40°C) of the thermotropic transition of surfactant membranes was observed by confocal microscopy of GUVs produced from native pulmonary surfactant (NPS) or its fractions (NPSE, NPSL, NPSP), doped with 0.1 mol % each of the probes DiIC18 (*red*) and Bodipy-PC (*yellow-green*). The scale bar represents 10 μm for all images except that of the GUV from NPS and observed at 40°C, which has its own smaller scale bar (also representing 10 μm).

To explore the order/mobility of phospholipids in the different pulmonary surfactant membranes further, we used EPR of native pulmonary surfactant membranes doped either with phosphatidylcholine spin-labeled on C-4 of the *sn*-2 chain (4-PCSL) or with the corresponding stearic acid (4-SASL). The spin-label EPR spectra are shown in Fig. S1 in the Supporting Material. The outer hyperfine splitting ($2A_{max}$) from 4-PCSL and 4-SASL in surfactant membranes decreases progressively with increasing temperature, as a result of the increased phospholipid chain mobility at higher temperatures. However, there are no abrupt increases in splitting or sharpening of the spectra that would indicate a cooperative transition from ordered/immobilized to disordered/mobile states in the temperature range where transitions are detected by DSC or fluorescence microscopy. Further, there is no indication of coexistence of components with different mobility in the spectra from surfactant membranes labeled with 4-PCSL, at any temperature. Therefore, the dynamics of the lipid probes incorporated into the two regions must be similar, at least for segments of the acyl chains close to the phospholipid headgroups.

Fig. 4 compares the temperature dependence of $2A_{max}$, from EPR spectra of phospholipid probes with the nitroxide group closer to the headgroup, at C-4 or C-8 of the chain, or closer to the center of the bilayer at C-12 or C-16, in membranes of NPSE, NPSL or NPSP. All have similar thermotropic profiles when probed with 4-PCSL or 8-PCSL. Chain mobility increases progressively with increasing temperature, but with no indication of sharp transitions to more mobile states in any range. Close to the end of the chain, the 16-PCSL probe attains full, near-isotropic, rotational mobility at temperatures above 10°C. At the C-12 position of the chain, a region typically affected by transmembrane proteins, the spectra indicate near-isotropic rotation first at temperatures between 25 and 35–37°C. The exact point is difficult to estimate because the line widths (determined by the rate of motion) are comparable to the residual anisotropy. Relative line heights of 12-PCSL (see Fig. S2) confirm, more sensitively, the nearly isotropic motion above 25°C. At temperatures >30°C, the mobility of 12-PCSL is reduced in samples of NPSE, presumably by lipid-protein interactions. As for 4-PCSL, there was no indication of coexisting spectral components from lipid populations with different mobilities for any of the different chain positions.

A direct comparison of EPR spectra from different positional isomers of the spin probe at 37°C shows that, at

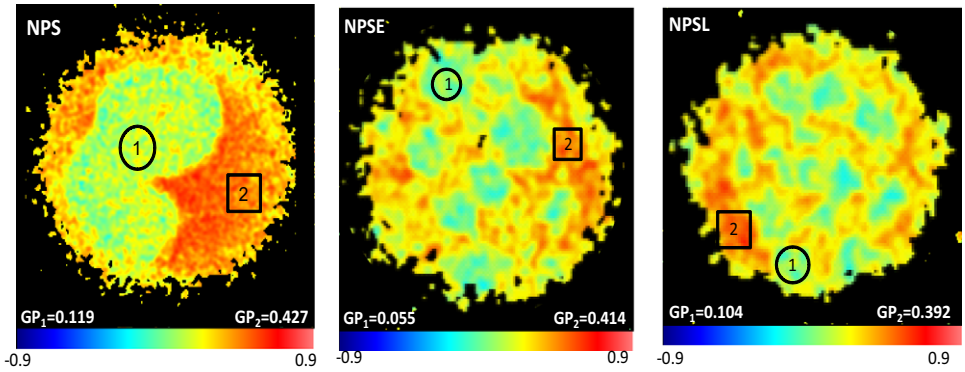

FIGURE 3 Packing and hydration properties of phases segregated in native pulmonary surfactant and membranes reconstituted from its fractions, as evaluated by the fluorescence of LAURDAN. Images have been taken by two-photon excitation confocal microscopy of GUVs from native pulmonary surfactant (NPS) or its fractions (NPSE, NPSL, NPSP), doped with 0.1 mol % of LAURDAN, at 20°C. Values of generalized polarization (GP) indicated are representative of measurements at the fluid disordered domains (*green*, 1) and at the fluid ordered background (*orange-red*, 2).

TABLE 2 GP of LAURDAN emission in the fluid ordered and fluid disordered regions of native pulmonary surfactant membranes or membranes reconstituted from its fractions

	LAURDAN GP*	
	Fluid ordered	Fluid disordered
NPS	0.37 ± 0.06	0.11 ± 0.02
NPSE	0.36 ± 0.04	0.07 ± 0.03
NPSL	0.34 ± 0.06	0.09 ± 0.02

GP, generalized polarization.
*Values are average ($N = 5$) ± SD. $T = 20°C$.

physiological temperature, the phospholipid chain segments near the headgroup region (sensed by 4- and 8-PCSL) have similarly restricted mobility in NPS, NPSE, and NPSL membranes and similar near-isotropic mobility at the terminal methyl ends of the acyl chains (i.e., 16-PCSL), (see Fig. S3). The spectrum of 12-PCSL in NPSE membranes corresponds to a region of the EPR timescale that is particularly sensitive to differences in amplitude and rates of rotational diffusion (e.g., Polnaszek et al. (25)) and is indicative of a markedly reduced lipid mobility compared with the spectra of protein-free surfactant bilayers, at temperatures both below and above physiological values (Fig. 5). Fig. 6 compares the full lipid chain flexibility gradient in the different surfactant membranes studied, at temperatures around the physiological values. Differences in $2A_{max}$ are higher at temperatures below 40°C, with the order of mobility being in general terms NPS < NPSE < NPSL ≤ NPSP. Maximal differences in mobility of the acyl chains are detected in the segments around carbon 12 of the chains (cf. above).

The information provided by spin-label EPR refers to the mobility of the phospholipid acyl chains, determined by rotational diffusion of the phospholipids and *trans-gauche* isomerizations about the C-C bonds in the chains. To obtain information about translational diffusion of phospholipids within the membrane plane, we have carried out experiments using proton pulse-field gradient NMR (pfg-NMR) with macroscopically oriented bilayers. Several studies have shown that macroscopically oriented membranes can be used as model systems when appropriately hydrated. Properties such as lipid transition temperatures, miscibility transition temperatures and lipid lateral diffusion coefficients agree with measurements carried out on giant liposomes and multilamellar dispersions (26–29), showing that the glass plate-assisted orientation does not change the bilayer properties. Pfg-NMR has been used to determine the translational diffusion coefficients (D_L) of phospholipids in several membrane models, and particularly to characterize the effect of cholesterol and the presence of liquid-ordered phases on the in-plane lateral diffusion of phospholipids in bilayers (30). The detection of two significantly different values of D_L is interpreted as the coexistence of two lipid populations with different diffusion properties, e.g., lipids in liquid-ordered and in liquid-disordered environments (28,30).

Our pfg-NMR data from surfactant preparations could always be fitted with just one phospholipid lateral diffusion coefficient, despite the fact that the corresponding membranes showed phase segregation under the confocal microscope (as seen in Figs. 2 and 3). Attempts to add a second lipid diffusion component did not result in any appreciable decrease in the normalized global sum of squares of errors and produced irrational spectral lineshapes and diffusion coefficients (see Oradd and Lindblom (21) for details on the procedures used to determine the number of components that can be resolved by this method). Fig. 7 shows representative plots of D_L for three types of surfactant membranes, as a function of

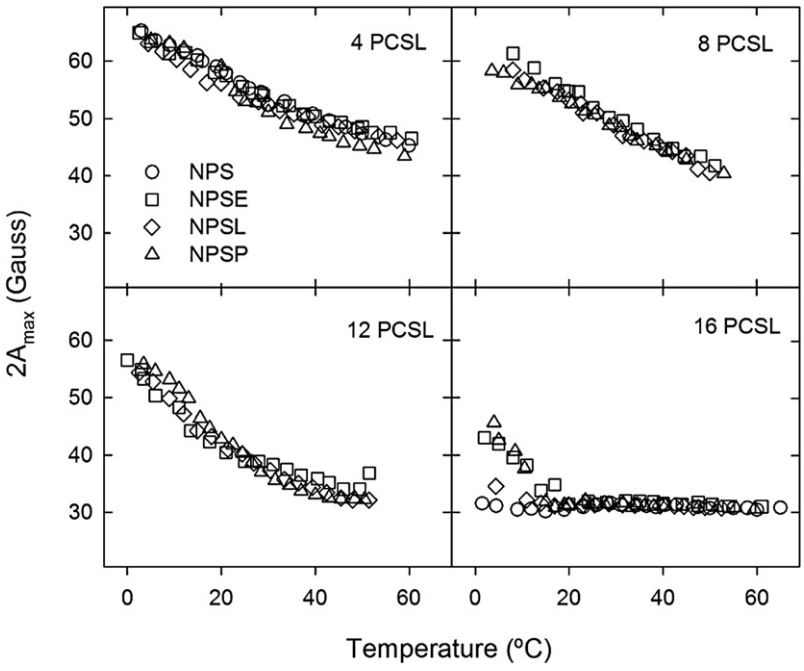

FIGURE 4 Temperature dependence of the mobility of different segments of the phospholipid acyl chains in native pulmonary surfactant and membranes reconstituted from its fractions Outer hyperfine splitting, $2A_{max}$, from the EPR spectra of native surfactant (NPS) or its reconstituted fractions (NPSE, NPSL, NPSP), has been plotted as a function of temperature for samples containing phosphatidylcholine probes spin labeled at different positions (*n*-PCSL) in the *sn*-2 acyl chain.

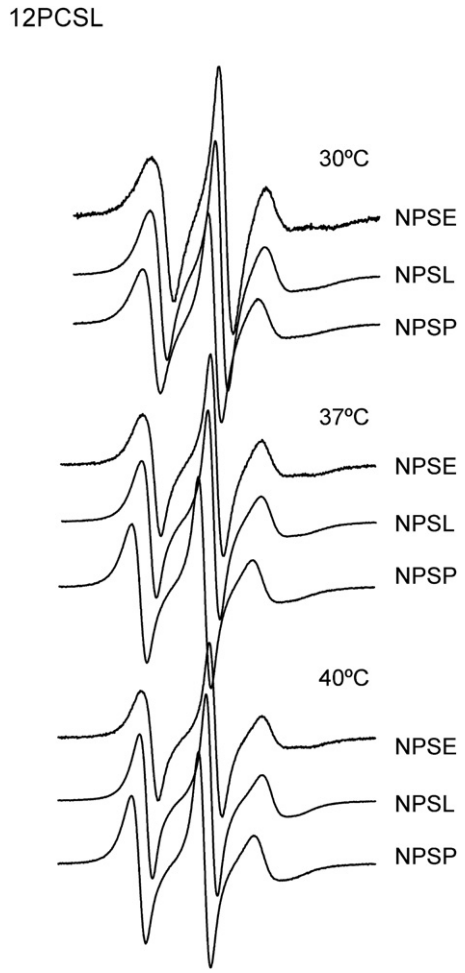

FIGURE 5 Effect of temperature on the dynamics of the 12-carbon segment of the phospholipid acyl chains in native pulmonary surfactant and membranes reconstituted from its fractions EPR spectra of native surfactant (NPS) or its reconstituted fractions (NPSE, NPSL, NPSP), doped with a phosphatidylcholine probe spin labeled at the 12-carbon of the *sn*-2 acyl chain, have been obtained and compared at the temperatures indicated.

temperature. Values of D_L at selected temperatures are summarized in Table S1. The absolute error in the measurements is estimated as $\pm 0.5\ \mu m^2/s$, based on the error estimation routine in the CORE software and the variability of results from several measurements on the same sample. Results from different sample preparations were qualitatively similar but with differences of up to $1\ \mu m^2/s$, reflecting the difficulty of obtaining the same lipid composition for different surfactant preparations. The values of D_L obtained from surfactant are in reasonable agreement with data from model membranes composed of mixtures of synthetic phospholipids and cholesterol (30). In general, the membranes investigated in this study show smaller differences in D_L, compared with the model membranes. This is probably a consequence of the more complex mixture of lipids in samples of biological origin. In all three systems, the phospholipid lateral diffusion coefficient increases progressively with increasing temperature. All temperature profiles for D_L show an inflection point at ~35°C, a temperature close to completion of the transition from the ordered state that was seen by calorimetry and fluorescence microscopy.

The lipid lateral diffusion coefficients determined in membranes of NPSE, which contain the hydrophobic proteins SP-B and SP-C, were lower than those determined at similar temperatures in membranes depleted of proteins, both in the presence and absence of cholesterol. This indicates that surfactant proteins SP-B and SP-C reduce the lateral mobility of phospholipids in surfactant membranes. In the absence of proteins, we detect a difference in the lateral diffusion of phospholipids between membranes with and without cholesterol that is larger at temperatures below the calorimetric transition. Below 32–35°C, the lateral diffusion of lipids in NPSP membranes is significantly faster than that in NPSL membranes. This is possibly due to the different character of the low-temperature phase coexistence in the presence (liquid-ordered/liquid-disordered type) and absence (gel/liquid-disordered type) of cholesterol. Above 35°C, the lateral diffusion coefficients of lipids in membranes with and without cholesterol are much closer, likely because both are dominated by liquid-disordered phases.

DISCUSSION

Considerable evidence suggests that lipids and proteins are sorted laterally in the membranes and films of pulmonary surfactant to form regions with important compositional, structural and dynamic differences (reviewed in Perez-Gil (8)). Compression of films with the full compositional complexity of pulmonary surfactant segregates domains of a condensed phase, which is enriched in the main surfactant phospholipid, the disaturated DPPC (7,31,32). An earlier model proposed that the saturated DPPC acyl chains, which permit high packing densities of the surfactant layers on compression, are strictly necessary to provide maximal stability at the end of expiration (5). Current models propose that the mechanical stability required for interfacial surfactant films to sustain the highest pressures—or lowest surface tensions—on compression arises from the alloy character of coexistence between fluid, disordered, but dynamic, regions and the mechanical resistance of more highly packed, ordered inclusions or domains (33,34). This picture, however, has been described so far only in static terms and does not consider the dynamic properties that can be of crucial importance for understanding pulmonary surfactant physiology.

The data presented here indicate that the two types of regions segregated in surfactant bilayers and films have a highly dynamic character. We have not been able to detect coexistence of phospholipid populations with different mobilities, as shown by EPR, in surfactant membranes that show phase separation under the fluorescence microscope. This suggests that the mobility of surfactant lipid chains does not differ greatly between the fluid disordered and fluid ordered

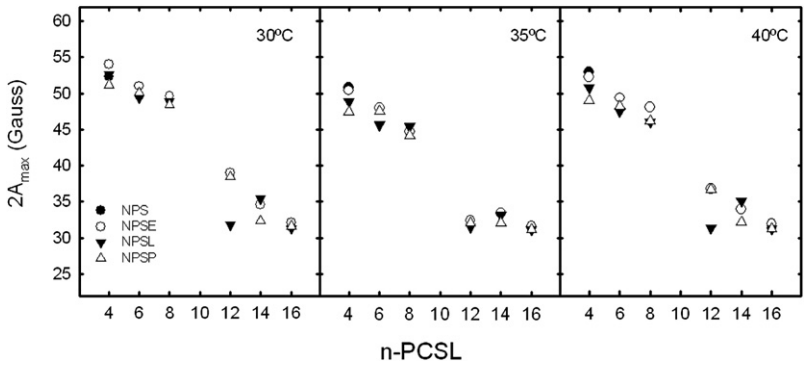

FIGURE 6 Effect of temperature on the chain flexibility gradient of native pulmonary surfactant and membranes reconstituted from its fractions. Outer hyperfine splittings, $2A_{max}$, from EPR spectra of *n*-PCSL in native surfactant (NPS) or its reconstituted fractions (NPSE, NPSL, NPSP) are plotted as a function of position, *n*, of the spin label in the *sn*-2 acyl chain, for the temperatures indicated.

regions, or that exchange of phospholipid molecules between these two types of region is faster than the difference in hyperfine splittings of their EPR spectra, which is maximally on the order of 10^8 s^{-1}. Resolvable differences in lipid mobility between coexisting liquid-ordered and liquid-disordered regions of sphingomyelin/cholesterol membranes have been reported from EPR spectra (35), indicating that the spin-labeled lipids can certainly partition into and probe the two types of phases (24). This, therefore, suggests that the phases segregated in pulmonary surfactant are more dynamic or more heterogeneous than those resolved in a canonical l_o-l_d coexistence.

Pfg-NMR shows heterogeneity of lateral diffusion coefficients in membranes that exhibit canonical coexistence of liquid-ordered and liquid-disordered phases (30). Lipids in the liquid-ordered phase have a slower rate of translational diffusion than those in liquid-disordered regions. These NMR experiments find no evidence for more than one lipid lateral diffusion coefficient in any of the surfactant membranes studied. One reason for this can be that the lateral mobility of the lipids is similar in the two phases, making it difficult to resolve two diffusion coefficients. If the diffusion coefficients differ by less than a factor of two, this might not be detected, especially if the fraction of one of the components is small. Thus, if the slower diffusion in the fluid ordered state is balanced by a similar reduction of D_L in the fluid disordered state, due to association of the hydrophobic proteins, the two-phase coexistence will not be detected. Adsorption of polylysine to cationic lipid membranes indeed induces a reduction in D_L comparable to that observed in liquid-ordered phases (A. Filippov, G. Orädd, and G. Lindblom, unpublished). Close examination of surfactant membrane structure on the nanometer scale by atomic force microscopy shows that the micrometer-sized ordered and disordered regions are really composed of much smaller ordered and disordered nanodomains (see Fig. S4). Lateral diffusion coefficients determined in the NMR experiments could then correspond to the average diffusion of lipid molecules among several ordered and disordered regions. The mean distance traveled by a lipid in the pfg-NMR experiment is $\sim(4D_L\Delta)^{1/2}$, which corresponds to ~1 μm. The domains shown in Fig. 2 are only slightly larger than 1 μm, and the nanoregions revealed by atomic force microscopy are even smaller, suggesting that pfg-NMR measurements could average lipid diffusion over the domain heterogeneity. However, this could not explain the detection of a single population of lipids on the much shorter timescale of spin-label EPR.

The effect of temperature on the dynamic properties of phospholipids in surfactant membranes, as analyzed in the different experiments shown here, illustrates how pulmonary surfactant lipid composition has probably evolved to sustain a specific dynamic behavior under physiological conditions. DSC, fluorescence, and NMR experiments show that pulmonary surfactant membranes, at physiological temperatures, are poised at the edge of a transition that has important consequences for the distribution of lipid and protein molecular species and their movement among the different surfactant structures. The potential impact of proximity of critical structural transitions to physiological conditions is probably unique to lung surfactant (36). Under these circumstances,

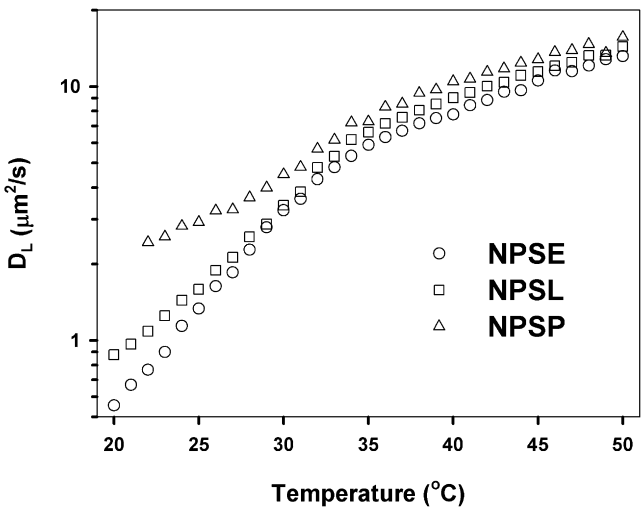

FIGURE 7 Effect of temperature on translational diffusion of phospholipids in membranes reconstituted from fractions of pulmonary surfactant, as determined by pfg-NMR. Temperature dependence of the lateral diffusion coefficient (D_L) of phospholipids has been analyzed in aligned planar membranes reconstituted from whole pulmonary surfactant organic extract (NPSE), and from the organic extract depleted of proteins (NPSL) or depleted of both proteins and cholesterol (NPSP).

surfactant structures could display critical behavior, facilitating generation and transmission of local membrane perturbations in response to, for instance, interfacial compression. In contrast to the thermotropic behavior of much simpler systems (17), the EPR spectra of natural surfactant mixtures do not show marked differences in intramolecular lipid dynamics when comparing temperatures above and below the thermotropic transition. This indicates that surfactant structures are similarly highly dynamic at the molecular level, independent of their macroscopic behavior. The reason for maintaining a dynamic surfactant structure close to such a transition has still to be established. One possibility is that environmental variables such as exposure to air, dehydration or compression during the breathing cycle, could allow surfactant to form surface films with a gradient of structural properties, ranging from relatively ordered, mechanically stable layers on the air-exposed side to very flexible membrane structures on the water/epithelial surface side, where the surface film has to integrate with newly secreted surfactant structures.

Finally, the data presented here allow some discussion of the possible role of cholesterol and the hydrophobic proteins SP-B and SP-C in modulating the dynamic properties of surfactant structures. Several recent studies have focused on the effect of cholesterol on the surface activity of pulmonary surfactant and concluded that surfactant can contain maximally ~10% of cholesterol by mass with respect to phospholipid without significant loss in ability to reach and sustain very low surface tensions (37). Contents of cholesterol higher than this are deleterious to surfactant function. Along the same lines, surfactant from ARDS patients has been found to contain abnormally high proportions of cholesterol, which is proposed as one of the reasons for its poor performance and a contribution to respiratory dysfunction (38). Our data suggest that the dynamic properties of surfactant could be optimized for a narrow range of working conditions, including lipid composition and temperature, among other possible important variables. It was found that the proportion of cholesterol changes in surfactant from animals and humans experiencing strenuous exercise (39). The level of cholesterol in surfactant could be subject to tight physiological regulation to fulfill the breathing requirements under different physiological conditions in a manner that could be specific of each different animal group (40). Alterations in surfactant compositional balance, e.g., the precise levels of cholesterol, could result in suboptimal performance and be a factor contributing to respiratory pathology, stressing the importance of optimizing the composition of the lipid component in the design of clinical surfactants.

Surfactant proteins have a substantial capacity for modulating the dynamic behavior of surfactant phospholipids in defined ways. Surfactant proteins reduce the enthalpy associated with thermotropic transitions in surfactant membranes, reduce the mobility of the lipid acyl chains, and cause a significant reduction in lateral diffusion rate of phospholipid species in the plane of membranes. All these alterations are probably related to perturbation by the proteins of phospholipid packing in surfactant structures. Protein structures segregated into dynamic membrane regions could limit the lateral diffusion of phospholipids in the membrane plane while facilitating their diffusion in the third dimension, crossing interconnected membranes and films that form part of a membrane surface phase (8). The results of this study suggest that this surface phase has an intrinsically dynamic behavior supported by an evolutionarily optimized lipid and protein composition.

SUPPORTING MATERIAL

A table and four figures are available at http://www.biophysj.org/biophysj/supplemental/S0006-3495(09)01216-8.

J.B.S was supported by a Lunbeck Foundation personal fellowship (Denmark). The NMR experiments were made possible through generous donations from the Knut and Alice Wallenberg Foundation. The EPR experiments were supported by the Max-Planck Society (Federal Republic of Germany).

This work was supported by the Spanish Ministry of Science (BIO2006-03130, CSD2007-00010), Community of Madrid (P-MAT-000283-0505), the Marie Curie Networks EST-007931, the European Commission (RTN-512229), the Forskningsrådet for Natur og Univers (L.A.B.), and the Danish National Research Foundation (which supports the MEMPHYS-Center for Biomembrane Physics).

REFERENCES

1. Daniels, C. B., and S. Orgeig. 2003. Pulmonary surfactant: the key to the evolution of air breathing. *News Physiol. Sci.* 18:151–157.
2. Zuo, Y. Y., R. A. Veldhuizen, A. W. Neumann, N. O. Petersen, and F. Possmayer. 2008. Current perspectives in pulmonary surfactant—inhibition, enhancement and evaluation. *Biochim. Biophys. Acta.* 1778:1947–1977.
3. Serrano, A. G., and J. Perez-Gil. 2006. Protein-lipid interactions and surface activity in the pulmonary surfactant system. *Chem. Phys. Lipids.* 141:105–118.
4. deMello, D. E. 2004. Pulmonary pathology. *Semin. Neonatol.* 9:311–329.
5. Goerke, J. 1998. Pulmonary surfactant: functions and molecular composition. *Biochim. Biophys. Acta.* 1408:79–89.
6. Ingenito, E. P., R. Mora, and L. Mark. 2000. Pivotal role of anionic phospholipids in determining dynamic behavior of lung surfactant. *Am. J. Respir. Crit. Care Med.* 161:831–838.
7. Discher, B. M., W. R. Schief, V. Vogel, and S. B. Hall. 1999. Phase separation in monolayers of pulmonary surfactant phospholipids at the air-water interface: composition and structure. *Biophys. J.* 77:2051–2061.
8. Perez-Gil, J. 2008. Structure of pulmonary surfactant membranes and films: the role of proteins and lipid-protein interactions. *Biochim. Biophys. Acta.* 1778:1676–1695.
9. Bernardino de la Serna, J., J. Perez-Gil, A. C. Simonsen, and L. A. Bagatolli. 2004. Cholesterol rules: direct observation of the coexistence of two fluid phases in native pulmonary surfactant membranes at physiological temperatures. *J. Biol. Chem.* 279:40715–40722.
10. Yan, W., S. C. Biswas, T. G. Laderas, and S. B. Hall. 2007. The melting of pulmonary surfactant monolayers. *J. Appl. Physiol.* 102: 1739–1745.

11. Lang, C. J., A. D. Postle, S. Orgeig, F. Possmayer, W. Bernhard, et al. 2005. Dipalmitoylphosphatidylcholine is not the major surfactant phospholipid species in all mammals. *Am. J. Physiol. Regul. Integr. Comp. Physiol.* 289:R1426–R1439.

12. Marsh, D., and A. Watts. 1982. Lipid-Protein Interactions. Wiley Interscience, New York.

13. Taeusch, H. W., J. B. de la Serna, J. Perez-Gil, C. Alonso, and J. A. Zasadzinski. 2005. Inactivation of pulmonary surfactant due to serum-inhibited adsorption and reversal by hydrophilic polymers: experimental. *Biophys. J.* 89:1769–1779.

14. Perez-Gil, J., A. Cruz, and C. Casals. 1993. Solubility of hydrophobic surfactant proteins in organic solvent/water mixtures. Structural studies on SP-B and SP-C in aqueous organic solvents and lipids. *Biochim. Biophys. Acta.* 1168:261–270.

15. Discher, B. M., K. M. Maloney, D. W. Grainger, C. A. Sousa, and S. B. Hall. 1999. Neutral lipids induce critical behavior in interfacial monolayers of pulmonary surfactant. *Biochemistry.* 38:374–383.

16. Bagatolli, L. A. 2006. To see or not to see: lateral organization of biological membranes and fluorescence microscopy. *Biochim. Biophys. Acta.* 1758:1541–1556.

17. Perez-Gil, J., C. Casals, and D. Marsh. 1995. Interactions of hydrophobic lung surfactant proteins SP-B and SP-C with dipalmitoylphosphatidylcholine and dipalmitoylphosphatidylglycerol bilayers studied by electron spin resonance spectroscopy. *Biochemistry.* 34:3964–3971.

18. Oradd, G., and G. Lindblom. 2004. Lateral diffusion studied by pulsed field gradient NMR on oriented lipid membranes. *Magn. Reson. Chem.* 42:123–131.

19. Tanner, J. E. 1970. Use of the stimulated echo in NMR diffusion studies. *J. Chem. Phys.* 52:2523–2526.

20. Stilbs, P., K. Paulsen, and P. C. Griffiths. 1996. Global least-squares analysis of large, correlated spectral data sets: application to component-resolved FT-PGSE NMR spectroscopy. *J. Phys. Chem.* 100: 8180–8189.

21. Oradd, G., and G. Lindblom. 2007. Lateral diffusion coefficients of raft lipids from pulsed field gradient NMR. *Methods Mol. Biol.* 398:127–142.

22. Keough, K. M., E. Farrell, M. Cox, G. Harrell, and H. W. Taeusch, Jr. 1985. Physical, chemical, and physiological characteristics of isolates of pulmonary surfactant from adult rabbits. *Can. J. Physiol. Pharmacol.* 63:1043–1051.

23. Marsh, D. 1990. Handbook of Lipid Bilayers. CRC Press, Boca Raton, FL.

24. Goni, F. M., A. Alonso, L. A. Bagatolli, R. E. Brown, D. Marsh, et al. 2008. Phase diagrams of lipid mixtures relevant to the study of membrane rafts. *Biochim. Biophys. Acta.* 1781:665–684.

25. Polnaszek, C. F., D. Marsh, and I. C. P. Smith. 1981. Simulation of the ESR spectra of the cholestane spin probe under conditions of slow axial rotation: application to gel phase dipalmitoyl phosphatidylcholine. *J. Magn. Reson.* 43:54–64.

26. Kahya, N. 2006. Targeting membrane proteins to liquid-ordered phases: molecular self-organization explored by fluorescence correlation spectroscopy. *Chem. Phys. Lipids.* 141:158–168.

27. Oradd, G., and G. Lindblom. 2004. NMR Studies of lipid lateral diffusion in the DMPC/gramicidin D/water system: peptide aggregation and obstruction effects. *Biophys. J.* 87:980–987.

28. Oradd, G., P. W. Westerman, and G. Lindblom. 2005. Lateral diffusion coefficients of separate lipid species in a ternary raft-forming bilayer: a Pfg-NMR multinuclear study. *Biophys. J.* 89:315–320.

29. Veatch, S. L., I. V. Polozov, K. Gawrisch, and S. L. Keller. 2004. Liquid domains in vesicles investigated by NMR and fluorescence microscopy. *Biophys. J.* 86:2910–2922.

30. Lindblom, G., and G. Oradd. 2009. Lipid lateral diffusion and membrane heterogeneity. *Biochim. Biophys. Acta.* 1788:234–244.

31. Discher, B. M., K. M. Maloney, W. R. Schief, Jr., D. W. Grainger, V. Vogel, et al. 1996. Lateral phase separation in interfacial films of pulmonary surfactant. *Biophys. J.* 71:2583–2590.

32. Nag, K., J. Perez-Gil, M. L. Ruano, L. A. Worthman, J. Stewart, et al. 1998. Phase transitions in films of lung surfactant at the air-water interface. *Biophys. J.* 74:2983–2995.

33. Keough, K. 2003. How thin can glass be? New ideas, new approaches. *Biophys. J.* 85:2785–2786.

34. Perez-Gil, J., K. Nag, S. Taneva, and K. M. Keough. 1992. Pulmonary surfactant protein SP-C causes packing rearrangements of dipalmitoylphosphatidylcholine in spread monolayers. *Biophys. J.* 63:197–204.

35. Collado, M. I., F. M. Goni, A. Alonso, and D. Marsh. 2005. Domain formation in sphingomyelin/cholesterol mixed membranes studied by spin-label electron spin resonance spectroscopy. *Biochemistry.* 44:4911–4918.

36. Trauble, H., H. Eibl, and H. Sawada. 1974. Respiration–a critical phenomenon? Lipid phase transitions in the lung alveolar surfactant. *Naturwissenschaften.* 61:344–354.

37. Gunasekara, L., S. Schurch, W. M. Schoel, K. Nag, Z. Leonenko, et al. 2005. Pulmonary surfactant function is abolished by an elevated proportion of cholesterol. *Biochim. Biophys. Acta.* 1737:27–35.

38. Gunther, A., C. Ruppert, R. Schmidt, P. Markart, F. Grimminger, et al. 2001. Surfactant alteration and replacement in acute respiratory distress syndrome. *Respir. Res.* 2:353–364.

39. Orgeig, S., H. A. Barr, and T. E. Nicholas. 1995. Effect of hyperpnea on the cholesterol to disaturated phospholipid ratio in alveolar surfactant of rats. *Exp. Lung Res.* 21:157–174.

40. Orgeig, S., and C. B. Daniels. 2001. The roles of cholesterol in pulmonary surfactant: insights from comparative and evolutionary studies. *Comp. Biochem. Physiol. A. Mol. Integr. Physiol.* 129:75–89.